GEOLOGY AND NOBLE METAL GEOCHEMISTRY OF THE POLARIS ULTRAMAFIC COMPLEX, NORTH-CENTRAL BRITISH COLUMBIA* (94C/5, 12)

By G.T. Nixon and J.L. Hammack;
J.N. Connelly, Memorial University of Newfoundland;
G. Case and W.P.E. Paterson, Consultants

KEYWORDS: Economic geology, Alaskan-type ultramafic complex, Polaris, structure, geochemistry, platinum group elements.

INTRODUCTION

The Polaris ultramafic complex is one of the largest Alaskan-type bodies in British Columbia, ranked second only to the Tulameen complex in the southern part of the province. Fieldwork and geochemical sampling at Polaris were conducted from fly camps during the last three weeks of August 1988, and preliminary results were released in Open File 1989-17 (Nixon *et al.*, 1989a). The complex was revisited for one week in August 1989 in order to conduct more detailed mapping of intrusive relationships and collect additional geochemical samples. This report summarizes the results of the fieldwork and presents a compilation of over 200 previously published (Nixon *et al.*, 1989a) and new analyses for platinum group elements and gold, as well as "pathfinder" elements such as nickel, chromium, arsenic, antimony and sulphur.

The project area is covered at a scale of 1:250 000 by the Mesilinka map sheet (94C) and 1:50 000 base maps (94C/5 and 12). Aeromagnetic survey maps are also available in the smaller (Map 7777G-Fort Grahame) and larger (Maps 9074G and 9075G) scales respectively.

LOCATION AND ACCESS

The Polaris ultramafic complex (56°30'N, 125°40'W) is situated 10 kilometres northeast of Aiken Lake in the Omineca Mountains (Figure 3-5-1). Access is by dirt road stretching some 335 kilometres north from Fort St. James via Manson Creek and Germansen Landing, to reach Aiken Lake via a well-maintained gravel road leading to the Cheni mine in the Toodogonne River area. Alternatively, the area may be reached via scheduled flights from Smithers to the Sturdee airstrip situated approximately 130 kilometres northwest of Aiken Lake, and from there by helicopter. The complex underlies an area of approximately 45 square kilometres at the southern end of the Lay Range and is well exposed above treeline at altitudes between 1600 and 2200 metres. It takes its name from Polaris Creek, a tributary of Lay Creek, both of which drain the western margin of the ultramafic body and flow southwards into the Mesilinka River.

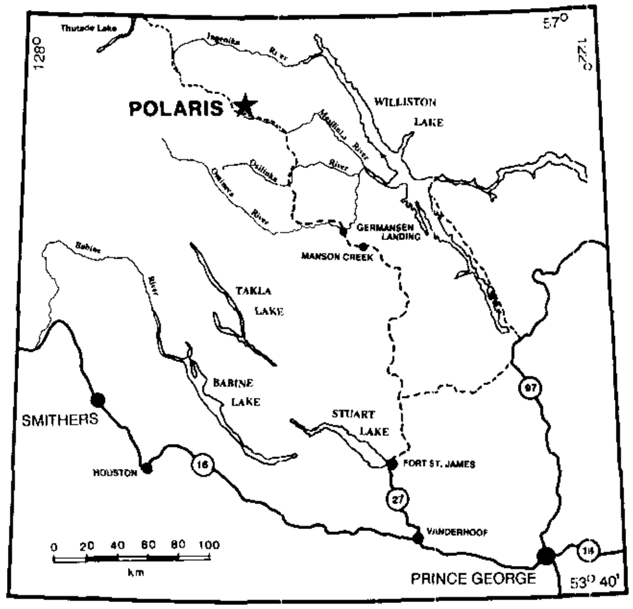

Figure 3-5-1. Location map of the Polaris ultramafic complex.

PREVIOUS WORK

The first systematic geologic mapping of the Aiken Lake area was completed by Armstrong (1946), Armstrong and Roots (1948), and Roots (1954). Earlier, Lay (1932) had examined many of the mineral prospects in the region.

The first detailed observations of the mafic and ultramafic rocks of the Polaris complex were made by Roots (1954). Modern petrologic studies and more detailed mapping of a host of Alaskan-type complexes were made later by Irvine (1974a, 1976). Prior to this paper, Irvine (1974a) and Foster (1974) presented the most complete descriptions of the Polaris complex. A revised edition of the geologic map previously released by Nixon *et al.* (1989a) is currently being prepared for publication (Nixon *et al.*, 1990).

GEOLOGIC SETTING

The Polaris ultramafic complex lies within the Omineca crystalline belt, a morphogeologic division of the Cordillera that straddles the boundary between ancestral North America and a collage of allochthonous tectonostratigraphic terranes (Quesnellia, Stikinia, Slide Mountain and Cache Creek) that

* This project is a contribution to the Canada/British Columbia Mineral Development Agreement.

amalgamated to form the Intermontane Superterrane before being accreted to the margin of the North American craton in the Mesozoic (Wheeler and McFeely, 1987). The Polaris complex is the largest of a number of Alaskan-type bodies that intrude Quesnellia (Figure 3-5-2). At this latitude, the Quesnel terrane is bounded on the west by Stikinia along the line of the Pinchi-Ingenika dextral fault system (Gabrielse, 1985; Wheeler *et al.*, 1988). Its eastern boundary is marked by the Swannell fault which places Upper Proterozoic rocks of the Ingenika Group, part of the pericratonic Kootenay Terrane (Wheeler *et al.*, 1988), in thrust contact with Quesnellia (Bellefontaine, 1989).

Arc-related augite-phyric flows, pyroclastic and epiclastic rocks of the Upper Triassic Takla Group characterize the Quesnel Terrane but are also found farther west in Stikinia (Figure 3-5-2; Richards, 1976a, b; Monger, 1977; Monger and Church, 1977). With the exception of the Menard complex (Nixon *et al.*, 1989b), all of the Alaskan-type bodies lie within Quesnellia, as presently defined, and all have been considered as comagmatic and coeval with Upper Triassic volcanism (Irvine, 1976). West of the Ingenika-Pinchi fault system, rocks of the Takla Group are metamorphosed to the zeolite or prehnite-pumpellyite facies whereas correlative lithologies to the east exhibit greenschist-grade assemblages (Richards, 1976b; Monger, 1977).

Mafic and ultramafic rocks of the Polaris complex are hosted by the Lay Range assemblage, a structurally complex sequence of arc-derived, predominantly clastic and volcaniclastic rocks that have been metamorphosed to greenschist or lower amphibolite grade (Monger, 1973, 1977; Richards, 1976a, b; Irvine, 1974a). These strata have been tentatively correlated with the Upper Devonian to Upper Permian Harper Ranch Group that forms the basement of Quesnellia in southern British Columbia (Monger *et al.*, in press).

The age of the Polaris complex is not well established. Potassium-argon dates on biotite and hornblende in a peridotite have yielded Jurassic isotopic ages of 167 ± 9 (2σ) and 156 ± 15 Ma (Wanless *et al.*, 1968). These dates have been considered too young by most workers who have stressed the spatial and petrological associations of Alaskan-type ultramafic complexes in British Columbia with Upper Triassic Takla-Nicola-Stuhini volcanic rocks of Quesnellia and Stikinia (*e.g.* Monger, 1973; Irvine, 1974a, 1976; Woodsworth *et al.*, in press). Uranium-lead dating is currently in progress in an attempt to firmly establish the age of the complex.

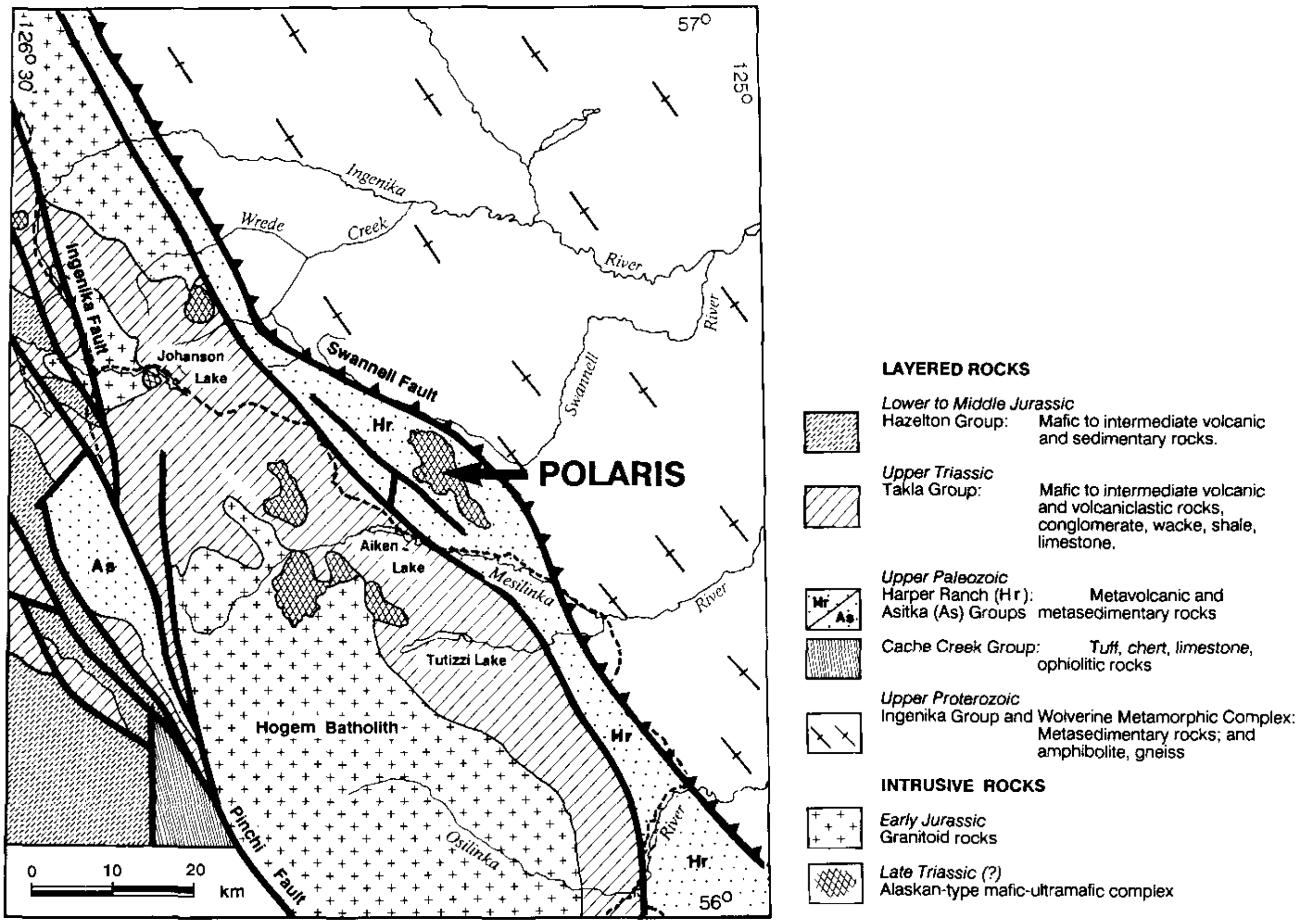

Figure 3-5-2. Geologic setting of the Polaris ultramafic complex (modified after Irvine, 1974; Monger, 1977; and Richards, 1976b).

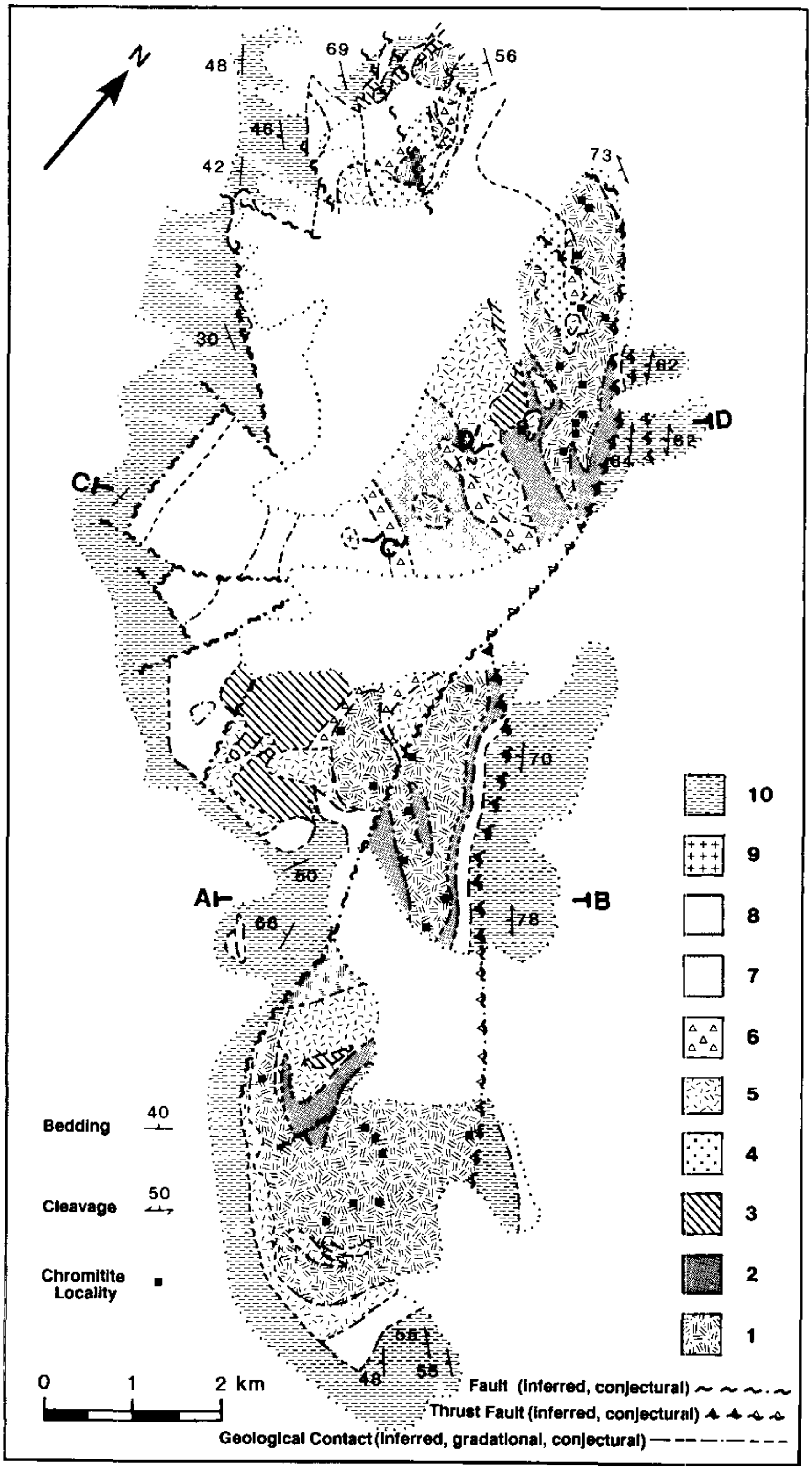

Figure 3-5-3. Generalized geology of the Polaris ultramafic complex (modified after Nixon *et al.*, 1989a). Key to map units: 1, dunite; 2, olivine wehrlite; 3, wehrlite; 4, undifferentiated olivine wehrlite and wehrlite; 5, olivine clinopyroxenite and clinopyroxenite. 6, mixed clinopyroxenitic and wehrlitic (with minor dunite) unit; 7, hornblende clinopyroxenite, clinopyroxene hornblendite, hornblendite and minor gabbro; 8, gabbroic rocks; 9, syenite/leucomonzonite; 10, metasedimentary and metavolcanic rocks of the Lay Range assemblage (Harper Ranch tectonostratigraphic terrane). Crosses indicate chromitite localities. A-B and C-C′-D′-D indicate location of cross-sections in Figure 3-5-4.

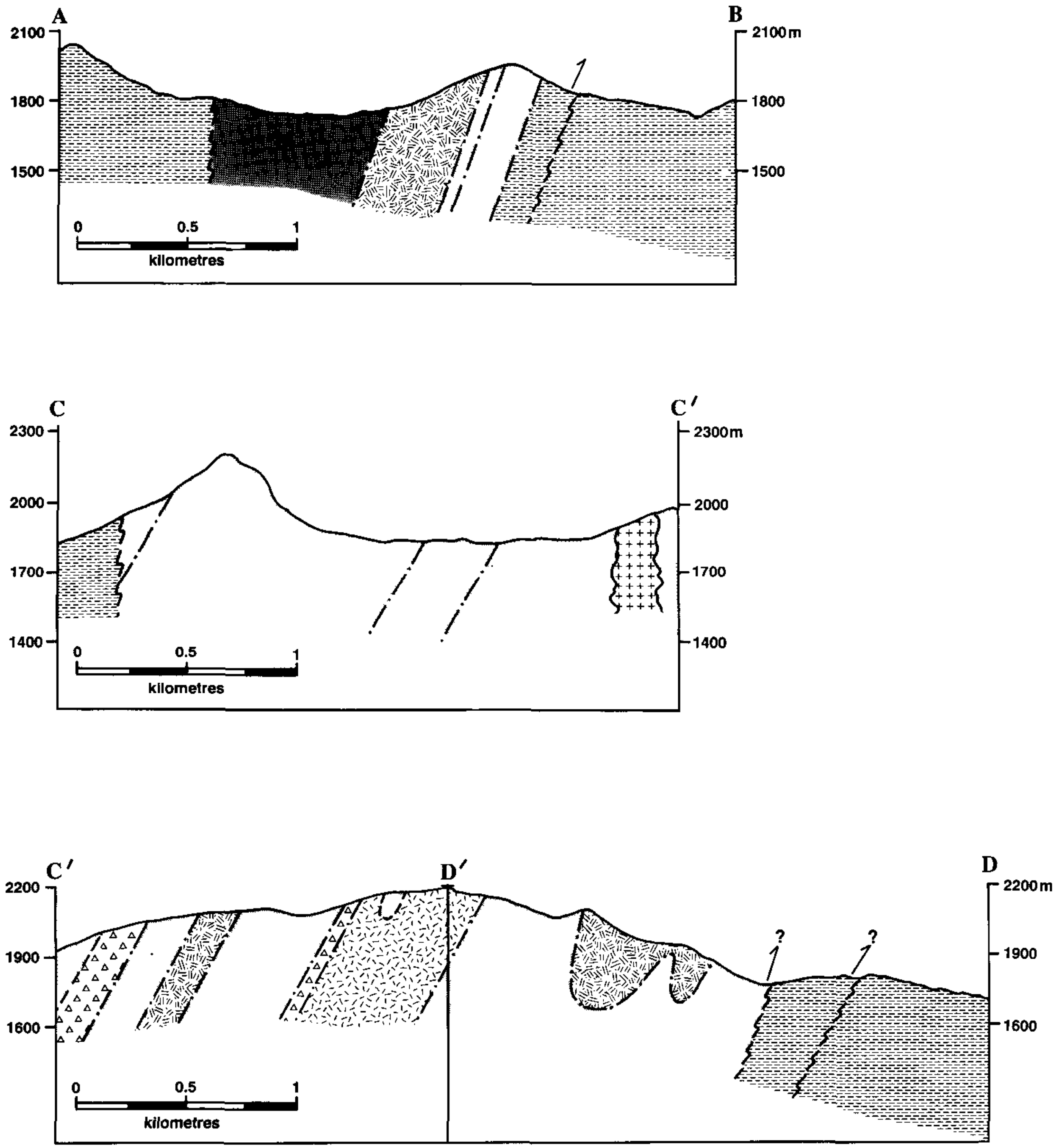

Figure 3-5-4. Schematic geologic cross-sections of the Polaris complex. *See* Figure 3-5-3 for locations. Note addition of hornblende clinopyroxenite unit in cross-section A-B.

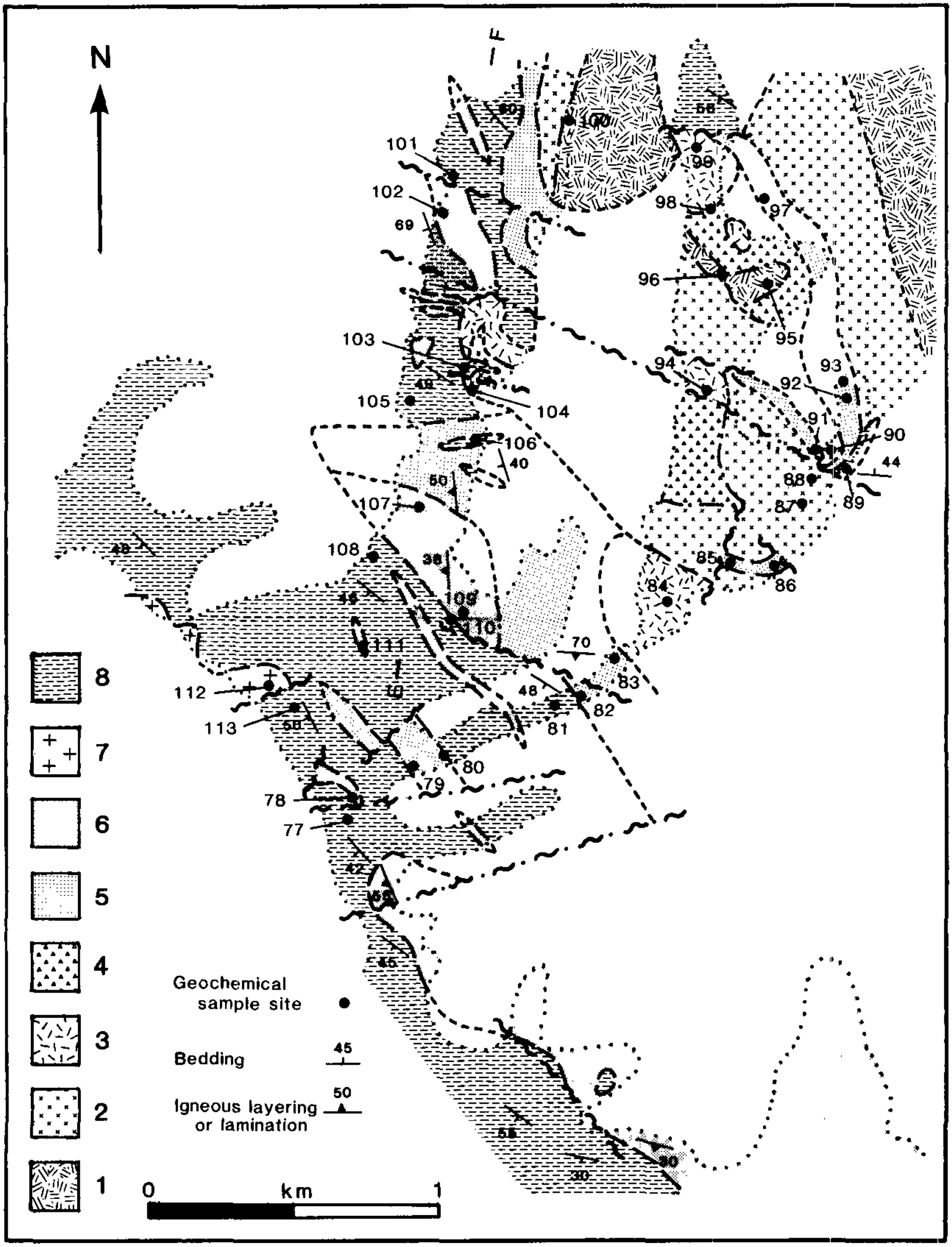

Figure 3-5-5. Generalized geology of the northwestern terminus of the Polaris ultramafic complex showing intrusive relationships and geochemical sample sites. Key to map units: 1, dunite, 2, undifferentiated olivine wehrlite and wehrlite; 3, olivine clinopyroxenite to clinopyroxenite; 4, mixed clinopyroxenitic and wehrlitic (with minor dunite) unit; 5, hornblende clinopyroxenite, clinopyroxene hornblendite, hornblendite and minor gabbro; 6, gabbroic rocks; 7, hornblende diorite; 8, metasedimentary and metavolcanic rocks of the Lay Range assemblage (Harper Ranch tectonostratigraphic terrane). E-F locates cross-section in Figure 3-5-6. Other symbols as in Figure 3-5-3.

COUNTRY ROCKS: LAY RANGE ASSEMBLAGE

Roots (1954) noted that rocks which host the Polaris complex form a moderately dipping (40°–50°) homoclinal sequence facing and inclined westwards. Monger (1973) recognized that the Lay Range assemblage is entirely fault-bounded and internally composed of a series of northwest-trending fault slices. Carbonates at the crest of the Lay Range northwest of the ultramafite have yielded mid-Pennsylvanian fossils, although younger Paleozoic or lowermost Mesozoic rocks may well exist (Monger, 1973; Monger and Paterson, 1974).

The immediate hostrocks of the Polaris complex comprise thickly to thinly bedded argillites, siltstones, sandstones, and minor carbonates, lithic-crystal tuffs and massive lava flows (Figures 3-5-3 to 3-5-6). Grey-green thinly bedded or laminated volcanogenic siltstones and fine-grained wackes are well exposed along the western margin of the complex where they form some of the highest peaks. The strata dip consistently to the west and are extensively silicified. Sedimentary features such as graded bedding, channel scours, load and flame structures, and crosslaminations indicate tops to the west. Locally, the succession contains chocolate-brown mudstones and thin (less than 0.3 metre thick), lenticular, impure carbonates characterized by brown-weathering rinds. At one locality (77, Figure 3-5-5), a thin (0 to 4 metres thick) medium grey layer of crystal-rich, non-welded ash-flow tuff contains rip-up clasts (up to 12 centimetres in length) of grey-green siltstone that are weakly imbricated and preferentially oriented within the direction of flow. The top of the deposit is reworked and the basal part exhibits normal grading and has scoured underlying siltstones. Thus, it appears to have been emplaced in a subaqueous environment.

Country rocks exposed at the northeastern margin of the complex include black fissile argillite and phyllite with interbedded fine-grained lithic tuff and pale grey carbonate. To the south, massive, aphanitic to porphyritic lavas of mafic to intermediate composition lie in sheared contact with serpentinized dunite at the southeastern margin of the complex. These lavas locally enclose concentrations of cognate xenoliths (up to 8 centimetres across) of hornblende gabbro, hornblendite and feldspathic hornblendite in a hornblende-phyric host. These rocks appear to have hornblende-phyric andesitic counterparts occurring as dikes in Lay Range assemblage strata overlying the intrusion.

POLARIS ULTRAMAFIC COMPLEX

The Polaris ultramafic complex forms an elongate body 14 kilometres long by 4 kilometres across at its broadest point. Its northwesterly trending long axis is conformable with the regional structural grain. The northern and southern terminations of the body are largely obscured by glacial drift. Farther north in the Lay Range, thin ultramafic sill-like intrusions, presumably coeval with the Polaris complex, were mapped by Roots (1954). However, the complex does not appear to have a large subsurface extension, judging from its distinctive aeromagnetic anomaly.

All of the lithologies that characterize Alaskan-type complexes are well represented in the Polaris complex (Figures 3-5-3 to 3-5-6). These include dunite, olivine wehrlite and wehrlite, olivine clinopyroxenite and clinopyroxenite, hornblende clinopyroxenite, hornblendite, gabbroic rocks, and late-stage pegmatites and finer grained feldspathic phases. A somewhat distinctive mineralogic feature is the appearance of phlogopitic mica in early cumulates, including dunite. Ultramafic lithologies are well exposed in the eastern and southern parts of the complex; gabbroic and hornblende-bearing rocks in the west.

ULTRAMAFIC ROCKS

DUNITE

The main mass of dunite forms northwest-trending ridges in the eastern half of the complex, and the floor and walls of a large cirque in the south. Dunite weathers tan to pale yellowish brown and forms smooth, blocky outcrops that typically lack a penetrative fabric. Joint planes are commonly lined with pale green to black serpentine that locally appears asbestiform. Fresh surfaces vary from dark greenish grey to black as the degree of serpentinization increases. Complete serpentinization, however, only occurs close to fault zones and, on the whole, olivines are well preserved. In thin section, the dunite is generally medium grained and composed of weakly serpentinized olivines (less than 3 milli-

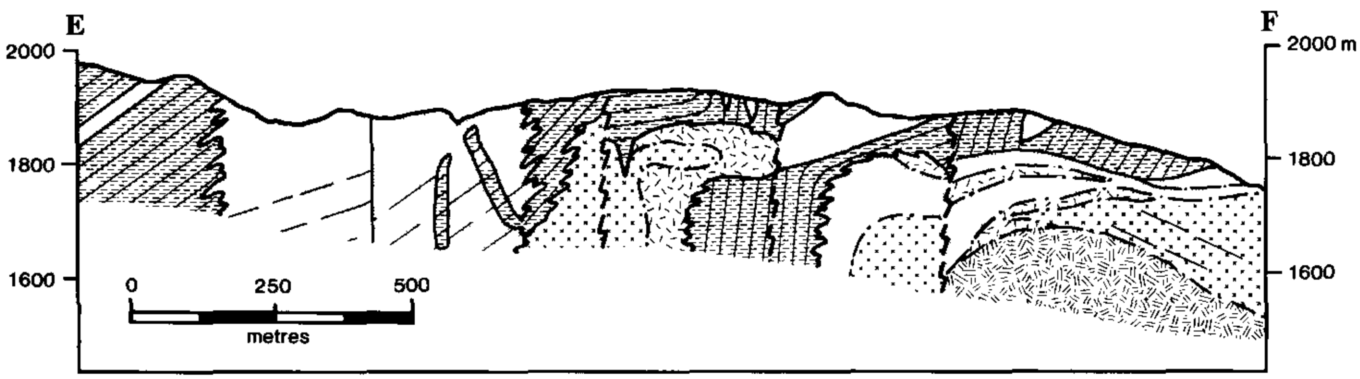

Figure 3-5-6. Schematic geologic cross-section of intrusive relationships at the northwestern end of the Polaris complex. *See* Figure 3-5-5 for location and key to map units. Attitude of bedding shown in host rocks; localized igneous layering or lamination depicted by dashed lines.

metres) and minor chromite (1 per cent by volume) that exhibit cumulate textures, accompanied by rare cumulus and intercumulus phlogopite.

CHROMITITE

Concentrations of chromite are confined to the dunite except for minor occurrences in olivine wehrlite adjacent to dunite (Figure 3-5-3). Chromitites occur as irregular pods, centimetre-scale schlieren, and millimetre-thick, planar to curved laminae. Schlieren commonly range from 6 to 15 centimetres in length and 0.5 to 4 centimetres in width; laminae can rarely be traced for more than 0.5 metre. Roots (1954) found more extensive chromitite horizons measuring almost 4 metres in length by 12 centimetres in width. Locally, coherent angular blocks of laminated chromitite up to 30 centimetres across are found juxtaposed in random orientation (Plate 3-5-1). In thin section, aggregates of chromite crystals commonly form networks or ring-like structures that partially to completely enclose cumulus olivines. Similar textures were documented by Clark (1978) from another Alaskan-type intrusion, the Turnagain River complex in northern British Columbia. The irregular geometry of podiform chromitites, pinch-and-swell nature of schlieren, and random orientation of layered chromitites are due to remobilization of previously deposited chromite-rich cumulates early in the crystallization history of the intrusion.

Plate 3-5-1. Disrupted block of layered chromitite in dunite cut by thin dunite dikes.

OLIVINE WEHRLITE AND WEHRLITE

Extensive outcrops of wehrlitic rocks are found in the northern and central parts of the complex and prompted subdivision into mappable units of olivine wehrlite (90 to 65 per cent olivine, 10 to 35 per cent clinopyroxene) and wehrlite (65 to 40 per cent olivine, 35 to 60 per cent clinopyroxene; nomenclature from Nixon, 1990). Wehrlitic lithologies weather pale brown to medium reddish brown and are massive to well jointed and weakly serpentinized; fresh surfaces are grey-green. These rocks commonly exhibit a knobby texture due to recessive weathering of olivine relative to clinopyroxene. In places, anhedral to subhedral megacrystic clinopyroxenes (up to 8 centimetres across) with well-developed poikilitic textures impart a distinctive lustre mottling to the outcrop (Plate 3-5-2). Olivines typically occur as cumulus crystals whereas clinopyroxenes exhibit intercumulus and cumulus textures. These primary silicates are accompanied by accessory chrome spinel and trace amounts of phlogopite. Rarely, wehrlitic mineralogy has formed by infiltration of clinopyroxene-rich magmas into an olivine-rich host, resulting in the formation of anastomizing three-dimensional networks of coarse-grained clinopyroxenite in the hostrock (Plate 3-5-3).

Plate 3-5-2. Megacrystic wehrlite exhibiting lustre mottling caused by subhedral poikilitic clinopyroxene. Magnet is 11 centimetres long. Photo by C. Nuttall.

Plate 3-5-3. Wehrlite formed by net veining of dunite near contact of clinopyroxenite and dunite bodies.

OLIVINE CLINOPYROXENITE AND CLINOPYROXENITE

Outcrops of olivine clinopyroxenite and clinopyroxenite are widely distributed throughout the ultramafic portion of the intrusion. Weathered surfaces are pale green to pale greyish green where enriched in clinopyroxene; olivine-rich areas appear rusty brown. The rocks are usually medium to coarse grained (3 to 10 millimetres) and grey-green on fresh surfaces. In pegmatitic zones, clinopyroxenes reach 8 centimetres in length and are rarely poikilitic. Locally, these zones contain olivine-rich areas or inclusions of wehrlite (less than 20 centimetres across) that are erratically distributed and render the outcrop mottled with rusty brown patches. In thin section, euhedral to subhedral clinopyroxenes are commonly schillered and exhibit inequigranular textures; most olivines appear subhedral and have cumulus or intercumulus textures. Phlogopite usually occurs as an accessory phase. Opaque oxides are notably reduced in abundance in olivine clinopyroxenites, and appear to be absent altogether in clinopyroxenites.

MIXED WEHRLITIC/PYROXENITIC UNITS

Mappable zones of intermixed olivine clinopyroxenite to clinopyroxenite and wehrlite to olivine wehrlite (and rarely dunite) are found locally near the margins of clinopyroxenite or wehrlitic bodies. They are particularly well developed in the central and northern parts of the intrusion (Figures 3-5-3 and 3-5-5). Contacts between the rock-types are generally sharp. The most common type of mixed unit comprises a chaotic assemblage of angular to subangular blocks of clinopyroxenite, ranging from less than one metre to tens of metres in size, enclosed by an olivine-rich host. This texture appears to have originated either by intrusion of clinopyroxenite magma into a semiconsolidated host, or by remobilization of zones of clinopyroxenite dike injection, similar to processes believed to be responsible for the disruption and redeposition of chromitite blocks. Another type of mixed zone is formed by concentrations of randomly oriented wehrlitic dikes cutting clinopyroxenite. The occurrence of mixed olivine-rich and pyroxenitic lithologies is also observed in the Tulameen complex (Nixon and Rublee, 1988) where they formed, in part at least, by slumping of coherent masses of dunite and/or clinopyroxenite cumulates that were plastically deformed during redeposition at lower levels in the magma chamber.

HORNBLENDE CLINOPYROXENITE AND HORNBLENDITE

This map unit comprises a gradation of rock types from hornblende clinopyroxenite through clinopyroxene hornblendite to hornblendite and feldspathic hornblendite. These hornblende-bearing ultramafic rocks are almost entirely restricted to the upper part of the complex where they are closely associated with gabbroic rocks. Hornblende clinopyroxenite occurs as a pale green to brownish green weathering, medium to coarse-grained rock studded with black hornblende crystals. It contains cumulus clinopyroxene, cumulus or intercumulus hornblende, locally abundant cumulus magnetite, accessory biotite and apatite, and intercumulus plagioclase appears in feldspathic variants. Hornblendite comprises a black, coarse-grained to pegmatitic texture with crystals reaching 8 centimetres in length. Locally, the rock exhibits a rude lineation, or a marked lamination of prismatic hornblende crystals with no directional fabric. A thin sill of megacrystic hornblende clinopyroxenite that intrudes roof rocks at the northwestern margin of the complex (Figure 3-5-5) locally displays well-developed centimetre-scale layering of cumulus subequant hornblende and clinopyroxene. Olivine-bearing hornblende clinopyroxenites are comparatively rare. One such unit occupies a narrow transition zone between dunite and hornblende clinopyroxenite at the zoned lower margin of the complex (Figure 3-5-4) and is distinguished by relatively abundant phlogopitic mica (5 per cent).

GABBROIC ROCKS

The gabbroic rocks comprise hornblende ± clinopyroxene gabbros and probably include undifferentiated dioritic phases carrying more sodic plagioclase. They are restricted to the margins of the complex and are most voluminous near the roof. They also form thin sills penetrating metasedimentary rocks of the Lay Range assemblage. Outcrops are typically lichen covered and dark grey weathering; fresh surfaces are medium grey to greenish grey depending on the degree of saussuritization of the feldspars. The rocks are usually massive, medium grained and equigranular. Centimetre-scale modal layering formed by alternating amphibole and plagioclase-rich horizons is observed locally and, near the contacts at least, is usually concordant with the attitude of bedding in the hostrocks. In thin section, the gabbroic rocks are composed of cumulus hornblende and rare clinopyroxene, cumulus to intercumulus plagioclase, accessory iron-titanium oxides, apatite and biotite, and sporadic secondary pyrite (less than 2 per cent).

Sills intruding the Lay Range assemblage have fine-grained chilled margins with rude columnar jointing or grade from medium-grained hornblende gabbro in the interior to hornblende porphyry at the contact. A narrow outer gabbroic zone at the lower margin of the complex locally displays an intense tectonic foliation that is locally mylonitic (described below) and concordant with that in metasedimentary hostrocks at the base of the intrusion.

DIKES AND VEINS

Dikes and veins of ultramafic to syenite/leucomonzonite or quartzofeldspathic composition are widespread in the Polaris complex, although there appears to be no systematic orientation to the pattern of dike intrusion. In large part, these dikes reflect the nature of, and temporal relationships between, major lithologic units.

Among the ultramafic rock types, centimetre to metre-wide dikes of olivine clinopyroxenite and clinopyroxenite are most common, and are found cutting dunite, olivine wehrlite and wehrlite (Plate 3-5-4). Dunite dikes, typically several centimetres in width, are only conspicuous where they penetrate chromitites (Plate 3-5-1); and thin olivine wehrlite to wehrlite dikes less than 0.5 metre wide transect dunite, wehrlitic and pyroxenitic units. The latter dikes locally exhibit concentrations of clinopyroxene crystals at their margins, a feature also documented at the Turnagain ultramafic complex (Clark, 1975). Thin (1 to 20 centimetres in width), medium to coarse-grained hornblendite to feldspathic hornblendite dikes have been observed cutting dunite, olivine clinopyroxenite, gabbroic rocks and metasedimentary strata of the Lay Range assemblage.

Leucocratic phases ranging from fine-grained, millimetre-width feldspathic veinlets to pegmatitic hornblende-biotite-feldspar ± quartz dikes and segregation pods several centimetres across are common within the gabbroic rocks and adjacent ultramafic units. In a ridge traverse along line D′-C′ (Figures 3-5-3 and 3-5-4), leucocratic dikes make their first appearance in dunite and wehrlitic lithologies and increase in abundance southward towards the gabbroic units. Composite dikes in the ultramafic rocks locally exhibit hornblendite margins and quartzofeldspathic cores; pegmatitic hornblende-feldspar-quartz segregation pods formed by ponding of residual liquids are also common in hornblende clinopyroxenites near the roof of the intrusion (Plate 3-5-5). The occurrence of silica-oversaturated differentiates in the Polaris complex may indicate late-stage contamination by siliceous wallrocks.

The overall sequence of dike intrusion, namely dunite, wehrlite, clinopyroxenite, hornblendite, gabbroic rocks and leucocratic residua, reflects the gross internal stratigraphy and general order of crystallization of major lithologic units in the complex. Locally ambivalent crosscutting relationships, such as those observed between olivine clinopyroxenite/clinopyroxenite and wehrlitic dikes, and hornblendite and gabbro, point to multiple intrusive events when magmas of a limited range of compositions coexisted.

Contact Relations and Intrusion Geometry

Steep contacts, rude internal zoning and the preservation of domical "roof" rocks at the northwestern end of the complex have previously been used to support a stock-like

Plate 3-5-4. Bifurcating wehrlite and clinopyroxenite dikes in dunite. Note thin offshoot of clinopyroxenite dike cutting wehrlite at left of hammer handle.

Plate 3-5-5. Pegmatitic hornblende-feldspar segregation pod in hornblende clinopyroxenite.

geometry for the intrusion (Roots, 1954; Irvine, 1974a; Foster, 1974). Detailed examination of contact relationships in the north confirms these crosscutting relationships (Figures 3-5-5 and 3-5-6). However, the elongate aspect of the complex, the nature of the western margin of the body where intrusive contacts are conformable with the strike and dip of metasedimentary hostrocks, the steep westward dip of zoned units at the eastern margin of the intrusion (Figure 3-5-4) and assymetrical nature of the zoning all suggest that the Polaris complex represents a high-level sill-like intrusion. Post-emplacement deformation has tilted the sill on end such that rocks forming the "roof" zone of earlier workers in fact represent wallrocks at the transgressive northern contact of the sill. Swarms of small gabbroic to pyroxenitic sills that intrude the roof zone to the west mimic the geometry of the larger intrusion.

Internal Stratigraphy

In general, the gross internal distribution of rock types is systematically disposed about the margins. Dunite and olivine-bearing pyroxenitic rocks are concentrated near the base of the intrusion whereas hornblende-bearing pyroxenites and gabbros are well developed near the roof. In the east-central part of the intrusion, the lower margin is progressively zoned from dunite through wehrlitic and olivine clinopyroxenitic lithologies to olivine-hornblende clinopyroxenites and hornblende-rich gabbroic rocks at the contact (Figure 3-5-4). Contact relationships among the major lithologic units are sharp to gradational.

Mechanism of Emplacement

Irvine (1974a; 1976) was struck by the internal zoning (albeit complex) and evidence for disruption of layered chromitites and clinopyroxenites by olivine-rich lithologies. He suggested that these features could be explained most satisfactorily by diapiric re-emplacement of hot, thickly stratified, olivine-rich cumulates in a semi-solid state during regional tectonism. We have difficulty with this hypothesis for a number of reasons. In the first place, relationships among the wehrlitic and pyroxenitic lithologies (*i.e.* mixed units of this report) are locally quite complex and exhibit a history of multiple intrusive events. As indicated earlier, the chaotic nature of mixed ultramafic lithologies and remobilized chromitite horizons can be explained adequately by periodic, syndepositional mass flux of cumulates to lower levels in the magma chamber, events perhaps triggered by earthquakes and episodic magma recharge. Furthermore, we have found no evidence for injection of dunite and wehrlitic lithologies into gabbroic and hornblende-rich lithologies which would be expected in Irvine's model; rather, intrusive relationships dictate the reverse. Also we note the general assymetry in the development of internal zoning; the lack of gabbroic rocks at all intrusive contacts; the widespread preservation of cumulate textures, and the general lack of penetrative fabrics both within and at the margins of the body, except where faulted. Moreover, why a high density mass of olivine cumulates would migrate "diapirically" to significantly higher levels in the crust rather than sink to the crust-mantle boundary is not explained. We therefore suggest that the internal stratigraphy of cumulates developed *in situ* (*i.e.*

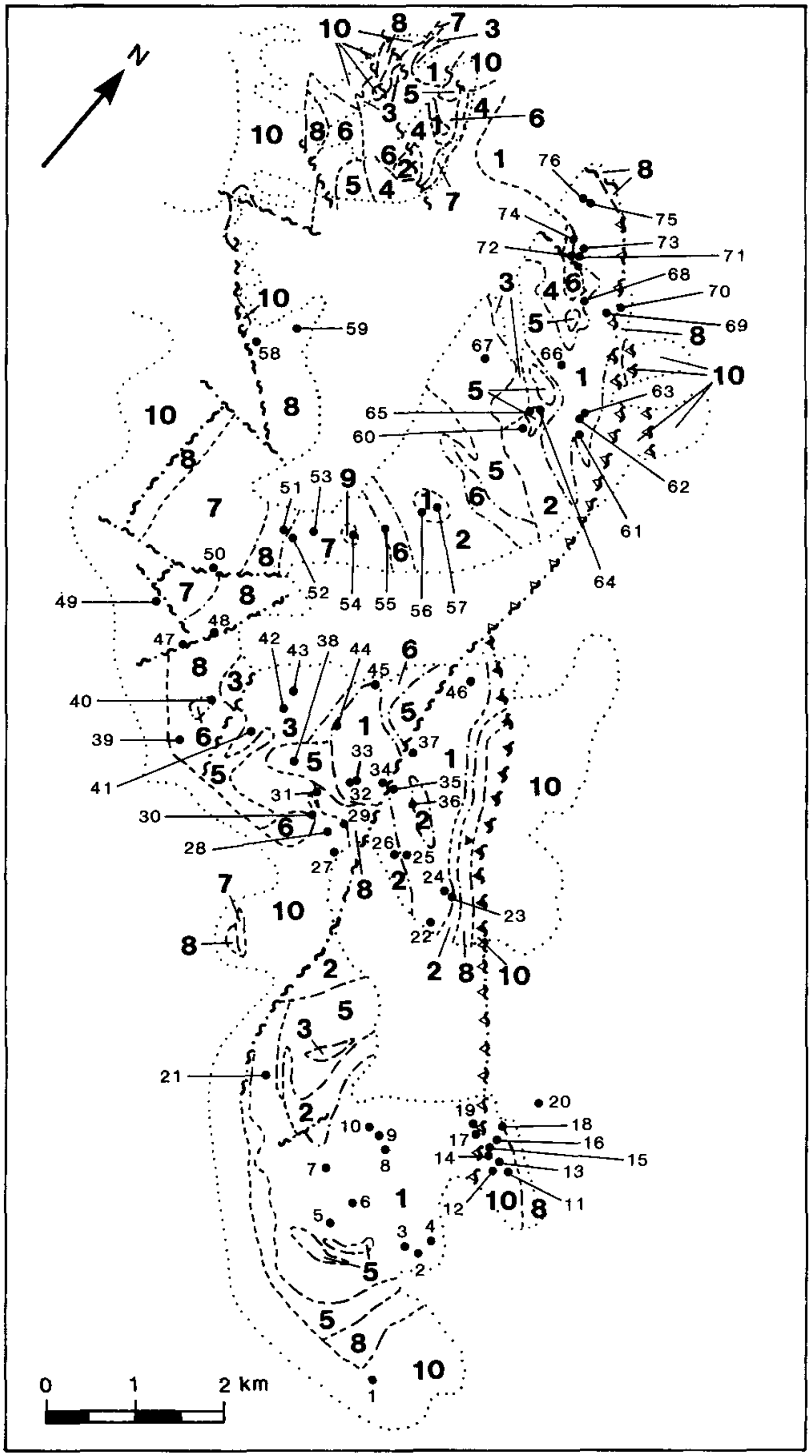

Figure 3-5-7. Location map of geochemical sample sites (also *see* Figure 3-5-5). Symbols and units as in Figure 3-5-3.

with respect to adjacent host rocks) essentially as we see it today, and probably represents the crystallization products of a subvolcanic magma chamber residing in the upper crust.

CONTACT AUREOLE

A contact aureole of amphibolite grade is well developed in rocks of the Lay Range assemblage at the margin of the intrusion. The maximum width of amphibolitic rocks is not accurately known, but has been estimated to extend on the order of 50 to 150 metres away from the contact (Irvine, 1974). The extent of hornfelsed rocks may be much greater than this, especially in the south (Roots, 1954).

In the north, metasedimentary rocks adjacent to the roof and margins of the complex have been recrystallized to an assemblage of hornblende, plagioclase, and quartz $\pm$ biotite $\pm$ potassium feldspar. The amphibolites exhibit no penetrative schistosity except where localized by faulting. Their finer grain size and preservation of relict stratification generally serves to distinguish these amphibolites from gabbroic and hornblende-rich ultramafic rocks of the intrusion.

At the southeastern extremity of the complex, serpentinized dunite lies in fault contact with black carbonaceous schists containing porphyroblasts of andalusite (chiastolite) up to 3 millimetres in length. Growth of andalusite appears to predate ductile movement in the shear zone and most likely formed in response to contact metamorphism. Andesitic lavas structurally underlying the phyllites lack a penetrative fabric but have undergone recrystallization of hornblende phenocrysts and groundmass consistent with amphibolite-grade metamorphism.

MINOR INTRUSIONS OF DUBIOUS AFFINITY

Intrusions that have uncertain relationships with the Polaris complex include a hornblende diorite sill-like body at the northwestern edge of the map area (Figure 3-5-5), a syenitic intrusion in the central part of the complex (Figure 3-5-3), and mafic dikes cutting metasedimentary rocks of the Lay Range assemblage. The dioritic body is a grey-brown weathering, fine to medium-grained rock, locally epidotized, with crystals of hornblende, plagioclase and minor potassium feldspar. The syenitic intrusion is a cream-weathering, greyish white coarse-grained rock comprising alkali feldspar (perthitic), minor hornblende, clinopyroxene and sphene, and trace amounts of biotite. It may be a late-stage differentiate of the Polaris complex that did not become silica-oversaturated for reasons yet to be determined. The dikes are dark greenish grey on weathered and fresh surfaces, and generally less than 2 metres in width, although they locally balloon to over 14 metres across. The thicker dikes have aphanitic chilled margins and hornblende-phyric interiors with up to 15 per cent phenocrysts. They are partly controlled by easterly oriented fault zones and are largely undeformed, appearing to postdate fault movement.

STRUCTURE AND METAMORPHISM

The Polaris complex is contained within a northwest-trending, southwest-facing and southwest-dipping homocline that represents a fault-bounded slice of Lay Range assemblage rocks. High-angle, northwest-trending faults are well exposed in the northern and eastern parts of the map area. They are commonly marked by schistose zones, crush breccias and quartz-carbonate alteration, and cut both the Polaris complex and its hostrocks. Most of these faults have displacements of unknown sense and magnitude.

Hostrocks overlying the intrusion, and wallrocks at the ends of the sill, lack a penetrative foliation. However, rocks resting structurally beneath the complex, especially lithologies adjacent to the eastern marginal fault, are generally highly schistose or mylonitic.

Metasedimentary rocks in ductile fault zones at the northeastern margin of the complex (cross-section D′-D, Figure 3-5-4), exhibit a single, well-developed slaty cleavage that is defined in thin section by biotite, muscovite, chlorite, quartz, plagioclase and minor carbonate. This mineral assemblage indicates that motion occurred during middle to upper greenschist facies metamorphism. Gabbroic rocks to the west have been inhomogeneously deformed and textures vary from massive to mylonitic with locally pronounced mineral lineations plunging steeply (60° to 70°) downdip to the northwest. In thin section, the mylonitic fabric is defined by amphibole, plagioclase, quartz, epidote, carbonate and chlorite (retrograde?) and deformation appears to have taken place under upper greenschist to lowermost amphibolite-grade conditions.

Oriented specimens were collected from metamorphosed volcaniclastic and sedimentary rocks farther south along the eastern marginal fault zone (cross-section A-B, Figure 3-5-4). C/S fabrics and shear bands observed in outcrop are defined in thin section by chlorite and biotite, and quartz and plagioclase have been dynamically recrystallized into subgrains. These textures indicate that mylonitization occurred during middle greenschist facies metamorphism. Kinematic indicators reveal that the hangingwall moved upward along southwest-dipping thrust planes. Mineral lineations plunging 65° to the northwest at the site of the C/S fabrics suggest that thrust movement, if parallel to the stretching direction, was toward the southeast. The eastern marginal fault zone continues farther south where it places dunite in thrust contact with andalusite-bearing schists that form part of the contact aureole (discussed above). A high-angle fault at the southwestern margin of the complex (cross-section A-B in Figure 3-5-4) also appears to be syntectonic with greenschist facies metamorphism.

From the preceding evidence, it is clear that major fault movements in the Lay Range took place during regional middle to upper greenschist metamorphism. The Polaris complex has been transported tectonically, together with its roof and most of its wallrocks, as an allochthonous thrust slice emplaced eastwards towards the craton, similar to other southwest-dipping, thrust-bounded packages mapped elsewhere in the Lay Range (Monger, 1973).

The eastward-verging structures in the Lay Range have counterparts in the Ingenika Group west of the Swannell fault, where they are represented by an early set of northwest-plunging, northeast-verging, tight to isoclinal folds (Bellefontaine, 1989). The Swannell fault represents a later, northeast-dipping, southwest-verging, imbricate thrust zone and associated drag folds that emplaced variably metamorphosed miogeoclinal rocks on Quesnellia (Bellefontaine, 1989). The timing of this deformation corresponds with the collision between the Intermontane Superterrane and ancestral North America which probably began in the Middle Jurassic (Gabrielse and Yorath, in press).

ALTERATION AND MINERALIZATION

Fault zones in the Polaris complex and Lay Range assemblage are commonly affected by quartz-carbonate alteration and weather to a bright orange-brown rock locally enriched in limonite, hematite, goethite and sulphides (largely pyrite). Alteration of this type develops in faults of every orientation in every lithology, but appears best developed in northwesterly and easterly trending fault zones. In addition to quartz and ferrodolomite, Irvine (1974a) noted the presence of vesuvianite, and Roots (1954) records ankerite and mariposite. Sparse quantities of asbestiform serpentine are restricted to joint surfaces and faults.

The Polaris complex appears remarkably devoid of sulphide mineralization. The only sulphides of note are exposed in several small reddish brown weathering outcrops of pyroxenitic rocks in the central part of the complex (Locality 43 in Figure 3-5-7). Here, net-textured primary sulphides, largely pyrrhotite, form immiscible blebs (up to 25 per cent) in a medium-grained clinopyroxenite. Disseminated secondary pyrite occurs locally in hornblende-rich ultramafic rocks and gabbros in amounts up to 2 per cent.

Chromitite is surprisingly sparse for the apparent size of the dunite mass. For example, in the Tulameen complex, which is a larger body but has a lower proportion of exposed dunite, chromitite is much more abundant. Likewise, the Wrede Creek complex appears to have more chromitite per square kilometre of exposed dunite than the Polaris intrusion. In both of the latter Alaskan-type bodies, platinum group elements are associated with chromitite (Nixon and Rublee, 1988; Hammack *et al.*, 1990, this volume). Evidently, the apparent size of the dunite body is no guide to its chromite or platinoid potential (discussed below). Magnetite is confined to the hornblende-bearing ultramafic and gabbroic lithologies but rarely exceeds 5 to 10 per cent of the rock and is of little economic significance.

GEOCHEMISTRY

Analytical results for gold, platinum group and "pathfinder" elements in over 130 representative samples of the Polaris complex and its hostrocks are presented in Table 3-5-1. Sample localities are shown in Figures 3-5-5 and 3-5-7. Three different analytical methods were used in two independent laboratories: inductively coupled plasma (ICP) mass spectrometry, Acme Analytical Laboratories, Vancouver; instrumental neutron activation analysis (INAA), Institut National de la Récherche Scientifique, Université du Québec; and inductively coupled plasma emission spectrometry, also Acme Analytical Laboratories. Accuracy was checked by international and in-house standards, and analytical precision (and any nugget effect) monitored by hidden duplicates and internal standards. All samples were preconcentrated by fire assay from 30 gram (ICP) or 50 gram (INAA) splits of 200 grams of rock powder (-200 mesh).

"Pathfinder" elements include sulphur, nickel, chromium, arsenic and antimony. Sulphur is generally low in abundance, and reaches a maximum value of 4.2 weight per cent in a clinopyroxenite (Locality 43, Table 3-5-1 and Figure 3-5-7) that contains net-textured sulphides and has weakly anomalous abundances of platinum and palladium. The only other sulphur-rich samples of note (greater than 1 per cent sulphur) are gabbros and metasedimentary rocks which contain secondary pyrite and exhibit no enrichment in the noble metals. Nickel and chromium have relatively high abundances in ultramafic rocks, but the latter element is particularly sensitive to the abundance of chromite in olivine-rich rocks. The highest chromium abundances reflect chip samples of high-grade chromitite; the chromitiferous dunites represent composite samples of small chromitite schlieren and host dunite. Thus, if platinum group elements (PGE) are preferentially concentrated in chromitite, as in the case of the Tulameen complex (St. Louis *et al.*, 1986), and PGE-rich and PGE-depleted chromitites exist, there will be no simple correlation between the abundance of chromium and PGE in the sample population. The abundances of arsenic and antimony are generally low and show no correlation with PGE or gold.

The highest concentration of platinum (735 ppb) is found in chromitiferous dunite (Locality 22, Figure 3-5-3) and is accompanied by small but significant quantities of rhodium, ruthenium, iridium and osmium. Low abundances of sulphur, arsenic and antimony suggest that the PGE may be contained as discrete platinum-iron alloys as typifies the chromitite-PGE association in the Tulameen complex (St. Louis *et al.*, 1986; Nixon *et al.*, 1989c). The tenor of platinum in a duplicate analysis is over fourteen times lower, and is attributed to a nugget effect, which appears to influence other samples (*e.g.* GN-88-1039, Locality 66). Rarely, abundances of iridium and osmium seem anomalously high (*e.g.* GN-88-1055B, Locality 71) and may indicate the presence of iridium-osmium(-ruthenium?) alloys which have been documented in other Alaskan-type associations (Harris and Cabri, 1973; Cabri and Harris, 1975). Anomalously high platinum and palladium (greater than 200 ppb) occur in a clinopyroxenite dike in the central part of the complex (GN-88-4069A, Locality 33). In general, palladium remains near or below detection limits in chromitites and olivine-rich ultramafic rocks, and increases in abundance in hornblende-bearing and gabbroic rocks. This behaviour is accompanied by a concomitant decrease in the platinum:palladium ratio, similar to trends in other Alaskan-type complexes (*e.g.* Nixon *et al.*, 1989b).

Highly anomalous abundances of gold (greater than 100 ppb) occur in an andesitic dike intruding metasedimentary sequences adjacent to a fault zone (Locality 77, Figure 3-5-5); in hornblendite at the roof of the ultramafic complex (Locality 82); and in dunite near the margin of the intrusion (Locality 100). In fact, all of the gold anomalies (greater than 20 ppb) are confined to the extreme northwestern end of the complex. Almost without exception, they exhibit a strong spatial relationship with intrusive contacts, although some are close to faults, and appear to favour mafic lithologies. No correlation is evident between the abundances of PGE and gold, which is generally low within the complex, and the few quartz veins and quartz-carbonate alteration zones sampled

TABLE 3-5-1
ABUNDANCES OF NOBLE METALS AND "PATHFINDER" ELEMENTS
IN THE POLARIS ULTRAMAFIC COMPLEX AND ASSOCIATED ROCKS

Locality	Sample	S wt %	Ni (ppm)	Cr (ppm)	As (ppm)	Sb (ppm)	Pt (ppb)	Pd (ppb)	Rh (ppb)	Ru (ppb)	Re (ppb)	Ir (ppb)	Os (ppb)	Au (ppb)
POLARIS COMPLEX														
Chromitite and Chromitiferous Dunite														
62	GN-88-1032[1]	—	—	—	—	—	<1	<2	<2	—	—	—	—	<1.0
62	GN-88-1032[2]	<0.02	1500	257955	<1.0	<0.20	<5	<5	7	<10	<5	8.70	4.8	<1.0
66	GN-88-1039[1]	—	—	—	—	—	49	5	<2	—	—	—	—	<1.0
66	GN-88-1039[2]	<0.02	2036	102308	<1.0	<0.20	121	<5	16	24	<5	33.00	18.0	<1.0
68	GN-88-1053[1]	—	—	—	—	—	<1	<2	<2	—	—	—	—	<1.0
68	GN-88-1053[1]*	—	—	—	—	—	<1	<2	3	—	—	—	—	<1.0
68	GN-88-1053[2]	<0.20	1929	75107	<1.0	<0.20	<5	<5	6	10	<5	4.50	<3.0	<1.0
71	GN-88-1055B[1]	—	—	—	—	—	28	<2	<2	—	—	—	—	<1.0
71	GN-88-1055B[1]*	—	—	—	—	—	72	5	<2	—	—	—	—	<1.0
71	GN-88-1055B[2]	<0.02	1870	64710	<1.0	<0.20	75	<5	19	45	<5	88.00	51.0	<1.0
76	GN-88-1058A[1]	—	—	—	—	—	<1	<2	<2	—	—	—	—	2.0
76	GN-88-1058A[1]*	—	—	—	—	—	2	<2	<2	—	—	—	—	<1.0
76	GN-88-1058A[2]	<0.02	2036	49612	<1.0	<0.20	<5	<5	3	31	<5	3.30	<3.0	<1.0
76	GN-88-1058B[1]	—	—	—	—	—	2	<2	<2	—	—	—	—	<1.0
76	GN-88-1058B[2]	<0.02	2322	39182	<1.0	<0.20	<5	<5	4	<10	<5	2.20	<3.0	<1.0
25	GN-88-1074[1]	—	—	—	—	—	72	<2	<2	—	—	—	—	<1.0
25	GN-88-1074[2]	<0.02	2331	58402	<1.0	0.37	—	—	—	—	—	—	—	<1.0
22	GN-88-1089[1]	—	—	—	—	—	50	<2	<2	—	—	—	—	<1.0
22	GN-88-1089[2]	<0.02	1641	75803	<1.0	<0.20	735	<5	24	32	<5	43.00	19.0	<1.0
63	GN-88-1031[1]	—	—	—	—	—	<1	<2	<2	—	—	—	—	<1.0
63	GN-88-1031[2]	<0.02	1660	155744	<1.0	<0.20	<10	<5	7	24	6	5.40	<3.0	<1.0
69	GN-88-1052[1]	—	—	—	—	—	<1	<2	<2	—	—	—	—	<1.0
69	GN-88-1052[2]	<0.02	2080	135880	<1.0	<0.20	<10	<5	5	<5	<5	9.30	6.0	<1.0
36	GN-88-1069B[1]	—	—	—	—	—	5	5	<2	—	—	—	—	<1.0
36	GN-88-1069B[1]*	—	—	—	—	—	3	6	<2	—	—	—	—	2.0
36	GN-88-1069B[2]	<0.02	2176	27235	<1.0	<0.20	<5	<5	2	<10	<5	3.90	<3.0	<1.0
24	GN-88-1092[1]	—	—	—	—	—	4	<2	<2	—	—	—	—	<1.0
24	GN-88-1092[2]	<0.02	1896	29311	<1.0	<0.20	<5	<5	5	<15	<5	4.50	<3.0	<1.0
61	GN-88-2050[1]	—	—	—	—	—	<1	4	<2	—	—	—	—	<1.0
61	GN-88-2050[2]	<0.02	2024	224571	<5.0	<0.30	<10	<5	9	16	<5	10.00	5.0	<1.0
37	GN-88-2072[1]	—	—	—	—	—	<1	3	<2	—	—	—	—	2.0
37	GN-88-2072[2]	<0.02	2467	89573	<5.0	<0.30	<5	<5	14	12	<5	8.90	6.5	<1.0
46	GN-88-2073[1]	—	—	—	—	—	<1	<2	<2	—	—	—	—	<1.0
46	GN-88-2073[2]	<0.02	2692	28022	<5.0	<0.30	9	<5	5	<5	<5	4.50	<3.0	<1.0
44	GN-88-2077[1]	—	—	—	—	—	<1	<2	<2	—	—	—	—	<1.0
44	GN-88-2077[2]	<0.02	1803	211248	<5.0	0.36	<5	<5	12	39	<5	10.00	<3.0	<1.0
17	GN-88-2107A[1]	—	—	—	—	—	5	<2	<2	—	—	—	—	<1.0
17	GN-88-2107A[2]	<0.02	2282	65558	<5.0	<0.30	<10	<5	3	<15	<5	3.10	3.4	<1.0
21	GN-88-2113[1]	—	—	—	—	—	3	<2	<2	—	—	—	—	<1.0
21	GN-88-2113[2]	<0.02	2093	41928	<5.0	<0.30	<5	<5	6	<15	<5	27.00	15.0	<1.0
10	GN-88-3145[1]	—	—	—	—	—	<1	<2	<2	—	—	—	—	<1.0
10	GN-88-3145[2]	<0.02	1929	143079	<5.0	<0.30	<10	<5	9	<15	<5	11.00	9.3	<1.0
75	GN-88-4068[1]	—	—	—	—	—	6	<2	<2	—	—	—	—	2.0
75	GN-88-4068[2]	<0.02	1821	261896	<5.0	<0.30	15	<10	5	<15	<5	22.0	15.0	<1.0
5	GN-88-4098[1]	—	—	—	—	—	2	<2	<2	—	—	—	—	<1.0
5	GN-88-4098[2]	<0.02	2181	107468	<5.0	<0.30	<10	<5	11	<20	<5	21.00	12.0	<1.0
9	GN-88-4102[1]	—	—	—	—	—	3	<2	<2	—	—	—	—	<1.0
9	GN-88-4102[2]	<0.02	1974	48594	6.5	<0.30	9	<5	4	<20	<5	5.70	4.0	<1.0
8	GN-88-4103[1]	—	—	—	—	—	2	<2	<2	—	—	—	—	<1.0
8	GN-88-4103[2]	<0.02	2004	113463	<5.0	<0.30	18	<5	4	<20	<5	8.60	9.4	<1.0
Dunite														
72	GN-88-1054B[1]	—	—	—	—	—	<1	<2	<2	—	—	—	—	2.0
72	GN-88-1054B[2]	<0.02	1650	1213	1.1	0.25	<5	<5	2	<5	<5	2.70	<3.0	<1.0
71	GN-88-1055A[1]	—	—	—	—	—	<1	<2	<2	—	—	—	—	<1.0
71	GN-88-1055A[2]	<0.02	2228	4407	<1.0	<0.20	21	<5	<1	26	<5	5.20	<3.0	1.1
73	GN-88-1056A[1]	—	—	—	—	—	6	<2	<2	—	—	—	—	2.0
73	GN-88-1056A[2]	<0.02	1986	2339	<1.0	<0.20	<10	<5	2	25	<5	5.50	3.5	<1.0
74	GN-88-1057A[1]	—	—	—	—	—	4	<2	<2	—	—	—	—	<1.0
74	GN-88-1057A[2]	0.02	2293	2977	<1.0	<0.20	<10	<10	<1	22	<5	2.80	<3.0	<1.0
95	GN-88-2044[1]	—	—	—	—	—	<1	3	<2	—	—	—	—	<1.0
96	GN-88-2048A[1]	—	—	—	—	—	<1	<2	<2	—	—	—	—	<1.0
96	GN-88-2048A[2]	<0.02	1723	3635	<5.0	<0.30	<5	<15	<1	17	<5	0.92	<3.0	<1.0
19	GN-88-2106[1]	—	—	—	—	—	5	<2	<2	—	—	—	—	<1.0
19	GN-88-2106[2]	0.03	2367	3969	5.4	<0.30	<5	<5	<1	<5	<5	1.30	<3.0	<1.0
2	GN-88-4092A[1]	—	—	—	—	—	2	<2	<2	—	—	—	—	<1.0
2	GN-88-4092A[2]	0.07	1928	2952	<5.0	0.31	<5	<5	<1	<5	<5	0.90	<3.0	<1.0
6	GN-88-4097[1]	—	—	—	—	—	2	<2	<2	—	—	—	—	2.0
6	GN-88-4097[2]	<0.02	2448	28449	<5.0	<0.30	<5	<5	2	<15	<5	3.30	3.7	<1.0
100	GN-89-6220[3]	—	—	—	—	—	<1	<2	<2	—	—	—	—	122.0

Analytical methods: [1] Inductively coupled plasma mass spectrometry, Acme Laboratories, Vancouver; [2] Instrumental neutron activation, Institutè National de la Récherche Scientifique, Québec; [3] Inductively coupled plasma emission spectrometry, Acme Laboratories, Vancouver.
Detection limits: 1 ppb for Pt and Au; 2 ppb for Pd and Rh; neutron activation detection limits vary with sample composition.
* Duplicate analysis.

TABLE 3-5-1 —*Continued*
ABUNDANCES OF NOBLE METALS AND "PATHFINDER" ELEMENTS IN THE POLARIS ULTRAMAFIC COMPLEX AND ASSOCIATED ROCKS

Locality	Sample	S wt %	Ni	Cr	As	Sb	Pt	Pd	Rh	Ru	Re	Ir	Os	Au
			ppm				ppb							
Olivine Wehrlite and Wehrlite														
72	GN-88-1054A[1]	—	—	—	—	—	<1	<2	<2	—	—	—	—	<1.0
72	GN-88-1054A[2]	<0.20	2175	3661	<1.0	<0.20	17	<5	3	27	<5	2.00	<3.0	<1.0
36	GN-88-1069A[1]	—	—	—	—	—	<1	3	<2	—	—	—	—	<1.0
36	GN-88-1069A[2]	<0.02	2026	3281	<1.0	<0.20	<10	<10	<1	20	<5	0.98	<3.0	<1.0
26	GN-88-1075[1]	—	—	—	—	—	<1	<2	<2	—	—	—	—	<1.0
23	GN-88-1093A[1]	—	—	—	—	—	7	<2	<2	—	—	—	—	2.0
23	GN-88-1093A[1]*	—	—	—	—	—	3	<2	<2	—	—	—	—	3.0
23	GN-88-1093A[2]	<0.02	1744	1096	2.3	<0.20	13	<5	2	<5	<5	3.00	3.8	<1.0
45	GN-88-2076[1]	—	—	—	—	—	<1	<2	3	—	—	—	—	<1.0
45	GN-88-2076[2]	<0.02	2521	99916	<5.0	<0.30	<10	<5	11	21	<5	6.90	4.8	<1.0
60	GN-88-4060[1]	—	—	—	—	—	<1	<2	<2	—	—	—	—	<1.0
60	GN-88-4060[2]	<0.02	2025	94789	6.9	<0.30	<15	<5	6	<40	<5	5.20	<3.0	<1.0
32	GN-88-4070A[1]	—	—	—	—	—	7	<2	<2	—	—	—	—	<1.0
87	GN-89-8143[3]	—	—	—	—	—	2	<2	<2	—	—	—	—	3.0
73	GN-88-1056B[1]	—	—	—	—	—	3	4	<2	—	—	—	—	<1.0
73	GN-88-1056B[2]	<0.02	1199	5284	<1.0	<0.20	<20	<10	<1	23	<5	1.60	<3.0	1.2
30	GN-88-4080A[1]	—	—	—	—	—	2	12	<2	—	—	—	—	<1.0
30	GN-88-4080A[2]	<0.02	1148	2298	<5.0	<0.30	9	12	<1	<5	<5	0.56	<3.0	<1.0
7	GN-88-4101[1]	—	—	—	—	—	<1	<2	<2	—	—	—	—	<1.0
7	GN-88-4101[2]	<0.02	1100	2764	<5.0	<0.30	<5	<5	<1	<10	<5	0.54	<3.0	<1.0
104	GN-89-6201[3]	—	—	—	—	—	2	<2	<2	—	—	—	—	3.0
90	GN-89-8134[3]	—	—	—	—	—	3	<2	<2	—	—	—	—	<1.0
Olivine Clinopyroxenite and Clinopyroxenite														
74	GN-88-1057B[1]	—	—	—	—	—	<1	<2	<2	—	—	—	—	<1.0
74	GN-88-1057B[2]	<0.02	442	4157	<1.0	<0.20	<20	<10	<1	22	<5	0.95	<3.0	<1.0
34	GN-88-1063[1]	—	—	—	—	—	<1	<2	<2	—	—	—	—	<1.0
96	GN-88-2048B[1]	—	—	—	—	—	<1	<2	<2	—	—	—	—	<1.0
96	GN-88-2048B[2]	<0.02	359	1849	<5.0	<0.30	<10	<35	<1	<15	<5	<0.10	<3.0	<1.0
43	GN-88-2079[1]	—	—	—	—	—	45	22	<2	—	—	—	—	3.0
43	GN-88-2079[2]	4.24	556	726	<5.0	<0.30	53	25	<1	20	6	0.27	<3.0	3.2
88	GN-88-4042[1]	—	—	—	—	—	<1	<2	<2	—	—	—	—	<1.0
64	GN-88-4052[1]	—	—	—	—	—	5	<2	<2	—	—	—	—	<1.0
67	GN-88-4063A[1]	—	—	—	—	—	<1	<2	<2	—	—	—	—	<1.0
67	GN-88-4063A[2]	<0.02	249	1798	<5.0	0.46	<5	<5	<1	<5	<5	<0.10	<3.0	<1.0
33	GN-88-4069A[1]	—	—	—	—	—	239	285	<2	—	—	—	—	7.0
32	GN-88-4070B[1]	—	—	—	—	—	5	11	<2	—	—	—	—	<1.0
3	GN-88-4093[1]	—	—	—	—	—	2	7	<2	—	—	—	—	<1.0
3	GN-88-4093[2]	<0.02	529	2556	<5.0	<0.30	<5	<5	<1	<15	<5	0.20	<3.0	<1.0
98	GN-89-7130[3]	—	—	—	—	—	4	<2	<2	—	—	—	—	14.0
98	GN-89-7131A[3]	—	—	—	—	—	4	<2	<2	—	—	—	—	<1.0
99	GN-89-9173[3]	—	—	—	—	—	50	70	7	—	—	—	—	13.0
55	GN-89-9141[3]	—	—	—	—	—	<1	<2	<2	—	—	—	—	5.0
52	GN-89-9146B[3]	—	—	—	—	—	13	7	<2	—	—	—	—	8.0
94	GN-89-9169B[3]	—	—	—	—	—	<1	<2	<2	—	—	—	—	<1.0
35	GN-88-1064[1]	—	—	—	—	—	8	13	<2	—	—	—	—	2.0
85	GN-89-8139[3]	—	—	—	—	—	8	9	<2	—	—	—	—	5.0
Hornblende Clinopyroxenite, Clinopyroxene Hornblendite, and Hornblendite														
48	GN-88-1077[1]	—	—	—	—	—	5	<2	<2	—	—	—	—	2.0
48	GN-88-1077[2]	<0.02	<150	<150	5.9	1.80	9	9	<1	7	<5	3.10	<3.0	<1.0
79	GN-88-4031A[1]	—	—	—	—	—	11	35	<2	—	—	—	—	<1.0
79	GN-88-4031A[2]	<0.02	251	732	<5.0	<0.30	12	24	1	<5	<5	0.13	<3.0	<1.0
79	GN-88-4031C[1]	—	—	—	—	—	<1	5	<2	—	—	—	—	3.0
92	GN-88-4045[1]	—	—	—	—	—	14	44	<2	—	—	—	—	<1.0
30	GN-88-4080B[1]	—	—	—	—	—	2	16	<2	—	—	—	—	2.0
30	GN-88-4080B[2]	<0.02	258	675	<5.0	<0.30	8	14	<1	<10	<5	0.15	<3.0	1.1
111	GN-89-7143B[3]	—	—	—	—	—	13	12	<2	—	—	—	—	10.0
79	GN-89-9132B[3]	—	—	—	—	—	16	20	<2	—	—	—	—	24.0
79	GN-89-9132C[3]	—	—	—	—	—	6	8	<2	—	—	—	—	22.0
82	GN-89-9167B[3]	—	—	—	—	—	48	14	7	—	—	—	—	174.0
57	GN-89-9139A[3]	—	—	—	—	—	5	5	<2	—	—	—	—	9.0
56	GN-89-9140A[3]	—	—	—	—	—	11	<2	<2	—	—	—	—	2.0
86	GN-89-8133A[3]	—	—	—	—	—	7	12	<2	—	—	—	—	<1.0
50	GN-88-1080B[1]	—	—	—	—	—	4	<2	<2	—	—	—	—	2.0
83	GN-88-2040B[1]	—	—	—	—	—	8	18	<2	—	—	—	—	<1.0
83	GN-88-2040B[1]*	—	—	—	—	—	9	15	<2	—	—	—	—	<1.0
83	GN-88-2040B[2]	0.44	<150	<150	<5.0	<0.30	14	16	<1	17	<5	0.17	<3.0	<1.0
97	GN-88-2045[1]	—	—	—	—	—	3	11	<2	—	—	—	—	<1.0
97	GN-88-2045[2]	<0.02	<150	966	<5.0	<0.30	7	<10	<1	13	<5	0.14	<3.0	<1.0
38	GN-88-4082B[1]	—	—	—	—	—	<1	14	<2	—	—	—	—	<1.0
38	GN-88-4082B[2]	<0.02	167	228	<5.0	<0.30	7	13	<1	<5	<5	<0.10	<3.0	<1.0
40	GN-88-4086[1]	—	—	—	—	—	<1	18	<2	—	—	—	—	<1.0
40	GN-88-4086[1]*	—	—	—	—	—	<1	15	<2	—	—	—	—	<1.0
40	GN-88-4086[2]	0.02	<150	287	<5.0	<0.30	6	10	<1	<5	<5	<0.10	<3.0	<1.0
93	GN-89-8147[3]	—	—	—	—	—	<1	<2	<2	—	—	—	—	2.0

Analytical methods: [1] Inductively coupled plasma mass spectrometry, Acme Laboratories, Vancouver; [2] Instrumental neutron activation, Institúté National de la Récherche Scientifique, Québec; [3] Inductively coupled plasma emission spectrometry, Acme Laboratories, Vancouver.
Detection limits: 1 ppb for Pt and Au; 2 ppb for Pd and Rh; neutron activation detection limits vary with sample composition.
* Duplicate analysis.

TABLE 3-5-1—*Continued*
ABUNDANCES OF NOBLE METALS AND "PATHFINDER" ELEMENTS
IN THE POLARIS ULTRAMAFIC COMPLEX AND ASSOCIATED ROCKS

Locality	Sample	S wt %	Ni	Cr	As	Sb	Pt	Pd	Rh	Ru	Re	Ir	Os	Au
			ppm				ppb							
Gabbroic Rocks														
70	GN-88-1050A[1]	—	—	—	—	—	2	<2	<2	—	—	—	—	2.0
50	GN-88-1080C[1]	—	—	—	—	—	<1	<2	<2	—	—	—	—	5.0
59	GN-88-2094[1]	—	—	—	—	—	3	8	<2	—	—	—	—	3.0
59	GN-88-2094[2]	0.01	<150	154	<5.0	<0.30	7	6	<1	18	<5	<0.10	<3.0	1.4
58	GN-88-2095[1]	—	—	—	—	—	<1	<2	<2	—	—	—	—	<1.0
58	GN-88-2095[2]	<0.02	<150	255	<5.0	<0.30	<5	<5	<1	22	<5	<0.10	<3.0	<1.0
18	GN-88-2100B[1]	—	—	—	—	—	2	<2	<2	—	—	—	—	11.0
18	GN-88-2100B[2]	2.72	<150	<150	<5.0	1.20	<5	<5	<1	19	<5	<0.10	<3.0	3.8
18	GN-88-2100C[1]	—	—	—	—	—	<1	<2	<2	—	—	—	—	<1.0
18	GN-88-2100C[2]	<0.02	<150	315	<5.0	0.64	<5	<5	<1	20	<5	<0.10	<3.0	<1.0
20	GN-88-2115[1]	—	—	—	—	—	4	<2	<2	—	—	—	—	<1.0
79	GN-88-4030B[1]	—	—	—	—	—	2	20	<2	—	—	—	—	2.0
81	GN-88-4036[1]	—	—	—	—	—	2	11	<2	—	—	—	—	4.0
81	GN-88-4036[2]	<0.02	<150	184	7.9	<0.30	7	11	<1	<5	<5	<0.10	<3.0	<1.0
29	GN-88-4073A[1]	—	—	—	—	—	<1	<2	<2	—	—	—	—	4.0
102	GN-89-6165[3]	—	—	—	—	—	7	7	<2	—	—	—	—	47.0
107	GN-89-6195[3]	—	—	—	—	—	8	9	<2	—	—	—	—	55.0
109	GN-89-7164[3]	—	—	—	—	—	9	9	<2	—	—	—	—	42.0
108	GN-89-6193B[3]	—	—	—	—	—	4	<2	<2	—	—	—	—	3.0
112	GN-89-9154[3]	—	—	—	—	—	8	9	<2	—	—	—	—	5.0
83	GN-88-2040A[1]	—	—	—	—	—	5	11	<2	—	—	—	—	<1.0
83	GN-88-2040A[2]	2.29	<150	746	<5.0	<0.30	11	14	<1	18	8	0.14	<3.0	<1.0
91	GN-88-4043A[1]	—	—	—	—	—	5	21	<2	—	—	—	—	9.0
31	GN-88-4072A[1]	—	—	—	—	—	5	16	<2	—	—	—	—	<1.0
31	GN-88-4072A[2]	0.30	<150	216	<5.0	<0.30	8	10	<1	<5	<5	<0.10	<3.0	<1.0
28	GN-88-4074[1]	—	—	—	—	—	<1	14	<2	—	—	—	—	<1.0
39	GN-88-4089[1]	—	—	—	—	—	<1	10	<2	—	—	—	—	<1.0
78	GN-89-9128C[3]	—	—	—	—	—	11	8	<2	—	—	—	—	27.0
51	GN-89-9147[3]	—	—	—	—	—	2	4	<2	—	—	—	—	4.0
80	GN-89-9148B[3]	—	—	—	—	—	11	9	<2	—	—	—	—	5.0
80	GN-89-9148B[3]*	—	—	—	—	—	11	9	<2	—	—	—	—	6.0
78	GN-89-9128A[3]	—	—	—	—	—	2	3	<2	—	—	—	—	38.0
Hornblende-Feldspar Pegmatites and Felsic Dikes														
42	GN-88-2078[1]	—	—	—	—	—	<1	<2	<2	—	—	—	—	<1.0
42	GN-88-2078[2]	<0.02	204	<150	<5.0	<0.30	<5	<5	<1	13	<5	<0.10	<3.0	<1.0
65	GN-88-4053D[1]	—	—	—	—	—	7	<2	<2	—	—	—	—	<1.0
29	GN-88-4073B[1]	—	—	—	—	—	2	<2	<2	—	—	—	—	<1.0
29	GN-88-4073B[2]	0.05	<150	<150	10.0	<0.30	<5	<5	<1	<5	<5	<0.10	<3.0	<1.0
27	GN-88-4076[1]	—	—	—	—	—	2	<2	<2	—	—	—	—	<1.0
41	GN-88-4085[1]	—	—	—	—	—	<1	<2	<2	—	—	—	—	<1.0
41	GN-88-4085[3]	<0.02	<150	<150	<5.0	<0.30	<5	<5	<1	8	<5	<0.10	<3.0	<1.0
105	GN-89-6188[3]	—	—	—	—	—	<1	<2	<2	—	—	—	—	60.0
82	GN-89-8123B-2[3]	—	—	—	—	—	2	<2	<2	—	—	—	—	<1.0
82	GN-89-8123B-1[3]	—	—	—	—	—	10	4	<2	—	—	—	—	<1.0
53	GN-89-9145Z[3]	—	—	—	—	—	2	<2	<2	—	—	—	—	<1.0
54	GN-89-9143[3]	—	—	—	—	—	<1	<2	<2	—	—	—	—	<1.0
LAY RANGE (HARPER RANCH) ASSEMBLAGE														
Metasedimentary and Metavolcaniclastic Rocks														
47	GN-88-2083[1]	—	—	—	—	—	<1	6	<2	—	—	—	—	<1.0
49	GN-88-2088[1]	—	—	—	—	—	2	4	<2	—	—	—	—	2.0
13	GN-88-2109[1]	—	—	—	—	—	<1	<2	<2	—	—	—	—	3.0
13	GN-88-2109[2]	1.32	<150	<150	5.5	<0.30	<5	<5	<1	<5	<5	<0.10	<3.0	1.6
11	GN-88-2110[1]	—	—	—	—	—	3	<2	<2	—	—	—	—	<1.0
101	GN-89-6162A[3]	—	—	—	—	—	<1	<2	<2	—	—	—	—	83.0
101	GN-89-6162B[3]	—	—	—	—	—	2	<2	<2	—	—	—	—	6.0
106	GN-89-6199[3]	—	—	—	—	—	9	5	<2	—	—	—	—	<1.0
1	GN-89-6225[3]	—	—	—	—	—	2	5	<2	—	—	—	—	3.0
110	GN-89-7147A[3]	—	—	—	—	—	19	20	<2	—	—	—	—	76.0
4	GN-89-8155[3]	—	—	—	—	—	2	<2	<2	—	—	—	—	12.0
103	GN-89-6202[3]	—	—	—	—	—	<1	4	<2	—	—	—	—	43.0
110	GN-89-7147B[3]	—	—	—	—	—	3	4	<2	—	—	—	—	5.0
89	GN-89-8136[3]	—	—	—	—	—	<1	4	<2	—	—	—	—	4.0
79	GN-89-9132A[3]	—	—	—	—	—	<1	<2	<2	—	—	—	—	19.0
80	GN-89-9148A[3]	—	—	—	—	—	2	6	<2	—	—	—	—	3.0
82	GN-89-9167A[3]	—	—	—	—	—	4	5	<2	—	—	—	—	4.0
Metavolcanic Rocks and Dikes														
14	GN-89-9175A[3]	—	—	—	—	—	<1	<2	<2	—	—	—	—	4.0
12	GN-89-9176[3]	—	—	—	—	—	<1	<2	<2	—	—	—	—	11.0
77	GN-89-9126C[3]	—	—	—	—	—	3	<2	<2	—	—	—	—	214.0
113	GN-89-9153A[3]	—	—	—	—	—	7	8	<2	—	—	—	—	13.0
QUARTZ VEINS AND QUARTZ-CARBONATE ALTERATION														
16	GN-88-2101[1]	—	—	—	—	—	<1	<2	<2	—	—	—	—	<1.0
15	GN-88-2108[1]	—	—	—	—	—	<1	<2	<2	—	—	—	—	2.0
84	GN-89-8126[3]	—	—	—	—	—	2	<2	<2	—	—	—	—	7.0

Analytical methods: [1] Inductively coupled plasma mass spectrometry, Acme Laboratories, Vancouver; [2] Instrumental neutron activation, Instituté National de la Récherche Scientifique, Québec; [3] Inductively coupled plasma emission spectrometry, Acme Laboratories, Vancouver.
Detection limits: 1 ppb for Pt and Au; 2 ppb for Pd and Rh; neutron activation detection limits vary with sample composition.
* Duplicate analysis.

are barren. These data suggest that circulating fluids, possibly driven by convective cooling at the margins of the intrusion, scavenged gold from Lay Range assemblage lithologies and deposited it near the contacts of the intrusion where mafic rocks acted as a chemical sink. The apparent spatial concentration of gold anomalies at the northwestern contacts is probably a reflection of sampling bias.

SUMMARY AND CONCLUSIONS

The Polaris ultramafic complex of north-central British Columbia provides an instructive example of an Alaskan-type intrusion. It represents one of the largest (45 square kilometres) of such bodies in the province, second only to the Tulameen complex in southern British Columbia. It is one of a number of Alaskan-type complexes that intrude the accreted terranes of Quesnellia and Stikinia and that are generally considered to represent the subvolcanic magma chambers of Late Triassic island arc volcanoes whose products comprise the Nicola, Takla and Stuhini Groups. Although spectacular mesoscopic layering such as that found at the classic locality of Duke Island (Irvine, 1974b) is nowhere developed, relationships with the country rocks, and between ultramafic and more differentiated gabbroic rocks, are well exposed. In addition, all typical Alaskan-type lithologies are represented, including dunite, chromitite, wehrlite, olivine clinopyroxenite, clinopyroxenite, hornblende clinopyroxenite, hornblendite, gabbros and more leucocratic pegmatitic phases. Cumulate textures are widespread and well preserved, and an interesting petrologic feature is the occurrence of cumulus and intercumulus phlogopite in early cumulates (dunite), indicative of relatively potassium-rich parental magmas. A potentially important economic consideration is the chromitite-platinoid association documented from other Alaskan-type intrusions.

Detailed mapping of the Polaris ultramafic complex and its environs has established that the body represents a westward-dipping, westward-facing transgressive sill that intruded metasedimentary and metavolcanic rocks of the Upper Paleozoic Lay Range assemblage (Harper Ranch tectonostratigraphic terrane) which forms the basement of Quesnellia. Intrusive contacts at the roof and margins of the sill are well exposed at the northwestern end of the complex. Here, minor coeval intrusions of gabbro and hornblende clinopyroxenite in the country rocks mimic the geometry of their larger counterpart.

The internal stratigraphy of the Polaris complex is well exposed in cross-section. The lower margin of the sill is zoned outward over a narrow interval from dunite through wehrlite and olivine clinopyroxenite to olivine-hornblende clinopyroxenite and hornblende gabbro. Dunite occupies much of the lower part of the intrusion, and, in a gross sense, is succeeded upward by thickly stratified wehrlitic cumulates and clinopyroxenites, hornblende-bearing clinopyroxenites and hornblendites, and hornblende-rich gabbroic rocks which are well developed near the roof of the intrusion. Contacts between the main lithologic units are sharp to gradational. On a more localized scale, evidence exists for complex multiple intrusive events between wehrlitic and pyroxenitic lithologies on the one hand, and between gabbroic and hornblende-rich ultramafic units on the other. Previously consolidated chromitite layers, and complex zones of intermixing of wehrlitic and clinopyroxenitic rocks, point to syndepositional remobilization of early cumulates by mass wasting processes which deposited them lower down in the magma chamber. The widespread remobilization of chromitite concentrations, combined with their scanty occurrence, do not bode well for commercial exploitation of chromite in these ultramafic rocks.

The Polaris complex is contained within a northwest-trending, westward-dipping homoclinal sequence of well-bedded country rocks with unambiguous sedimentary structures that face west. High-angle faults with predominantly northwesterly and westerly trends transect ultramafic and country rocks alike. A basal ductile thrust zone exposed at the eastern margin of the complex exhibits S/C fabrics and kinematic indicators which suggest tectonic transport to the east. The Polaris complex has therefore been tectonically uprooted and transported, together with its hostrocks, as an allochthonous slice, similar to the structure of rock packages documented in other parts of the Lay Range. Major faulting was active during middle to upper greenschist regional metamorphism which appears to be superimposed on a contact aureole of amphibolite grade. This deformation and regional metamorphism are probably related to the collision of accreted terranes of the Intermontane Belt, specifically Quesnellia, against the miogeocline of ancestral North America.

Lithogeochemical assays for platinum group elements, gold, and associated pathfinder elements yield some interesting but rather localized anomalies. Platinum attains a maximum abundance of 735 ppb in chromitite-bearing dunite, and is accompanied by minor iridium and osmium which reach maximum abundances of 88 and 51 ppb respectively. A sample of clinopyroxenite yields anomalously high platinum and palladium of 239 and 285 ppb respectively. The platinum group elements have no apparent correlation with the abundances of pathfinder elements suggesting that the platinoids may be contained as discrete platinum-iron or ruthenium-iridium-osmium alloys. Gold anomalies (20 to 214 ppb) show a preference for mafic lithologies at the margins of the ultramafic complex. This suggests that the mafic rocks may have acted as a chemical trap for mineralizing fluids circulating adjacent to the intrusion, and that the gold was derived from the country rocks.

ACKNOWLEDGMENTS

Fieldwork at the Polaris complex was funded by the Mineral Development Agreement between Canada and the Province of British Columbia. Exceptional support in the field was provided by Chris Ash and Carol Nuttall. We would also like to thank our expeditor, Sandy Jaycox of Jaycox Industries, and our helicopter pilot, Keith Buchanan of Northern Mountain Helicopters, for their caring, personal service. Special thanks to Tom Brooks of Canadian Helicopters for allowing us to use facilities at Sturdee airstrip and Johanson Lake. Last, but by no means least, thanks are extended to the crew of the Shasta camp for their extraordinary hospitality. Thanks to Brian Grant for reviewing the earlier, rude form of this manuscript.

REFERENCES

Armstrong, J.E. (1946): Aiken Lake (South Half), British Columbia; *Geological Survey of Canada*, Paper 46-11.

Armstrong, J.E. and Roots, E.F. (1948): Geology and Mineral Deposits of Aiken Lake Map Area, British Columbia; *Geological Survey of Canada*, Paper 48-5, 46 pages.

Bellefontaine, K.A. (1989): Tectonic Evolution of Upper Proterozoic Ingenika Group, North-central British Columbia; *B.C. Ministry of Energy, Mines and Petroleum Resources*, Geological Fieldwork 1988, Paper 1989-1, pages 221-226.

Cabri, L.J. and Harris, D.C. (1975): Zoning in Os-Ir Alloys and the Relation of the Geological and Tectonic Environment of the Source Rocks to the Bulk Pt:Pt + Ir + Os Ratio for Placers; *Canadian Mineralogist*, Volume 13, pages 266-274.

Clark, T. (1975): Geology of an Ultramafic Complex on the Turnagain River, Northwestern British Columbia; unpublished Ph.D. thesis, *Queen's University*, 453 pages.

——— (1978): Oxide Minerals in the Turnagain Ultramafic Complex, Northwestern British Columbia; *Canadian Journal of Earth Sciences*, Volume 15, pages 1893-1903.

Foster, F. (1974): History and Origin of the Polaris Ultramafic Complex in the Aiken Lake Area of North-central British Columbia; unpublished B.Sc. thesis, *The University of British Columbia*, 66 pages.

Gabrielse, H. (1985): Major Dextral Transcurrent Displacements along the Northern Rocky Mountain Trench and Related Lineaments in North-central British Columbia; *Geological Society of America Bulletin*, Volume 96, pages 1-14.

Gabrielse, H. and Yorath, C.J. (in press): Tectonic Synthesis, Chapter 18, *in* The Cordilleran Orogen: Canada, Gabrielse, H. and Yorath, C.J., Editors, *Geological Survey of Canada*, Geology of Canada, Number 4.

Hammack, J.L., Nixon, G.T., Wong, R.H. and Paterson, W.P.E. (1990): Geology and Noble Metal Geochemistry of the Wrede Creek Ultramafic Complex, North-central British Columbia; *B.C. Ministry of Energy, Mines and Petroleum Resources*, Geological Fieldwork 1989, Paper 1990-1, this volume.

Harris, D.C. and Cabri, L.J. (1973): The Nomenclature of the Natural Alloys of Osmium, Iridium, and Ruthenium Based on New Compositional Data of Alloys from Worldwide Occurrences; *Canadian Mineralogist*, Volume 12, pages 104-112.

Irvine, T.N. (1974a): Ultramafic and Gabbroic Rocks in the Aiken Lake and McConnell Creek Map-areas, British Columbia; *Geological Survey of Canada*, Paper 74-1A, pages 149-152.

——— (1974b): Petrology of the Duke Island Ultramafic Complex, Southeastern Alaska; *Geological Society of America*, Memoir 138, 240 pages.

——— (1976): Alaskan-type Ultramafic-Gabbroic Bodies in the Aiken Lake, McConnell Creek and Toodoggone Map-areas; *Geological Survey of Canada*, Paper 76-1A, pages 76-81.

Lay, R. (1932): Aiken Lake Area, North-central British Columbia; *B.C. Ministry of Energy, Mines and Petroleum Resources*, Bulletin 1, 32 pages.

Monger, J.W.H. (1973): Upper Paleozoic Rocks of the Western Canadian Cordillera; *Geological Survey of Canada*, Paper 73-1A, pages 27-28.

——— (1977): The Triassic Takla Group in McConnell Creek Map-area, North-central British Columbia; *Geological Survey of Canada*, Paper 76-29, 45 pages.

Monger, J.W.H. and Church, B.N. (1977): Revised Stratigraphy of the Takla Group, North-central British Columbia; *Canadian Journal of Earth Sciences*, Volume 14, pages 318-326.

Monger, J.W.H. and Paterson, I.A. (1974): Upper Paleozoic and Lower Mesozoic Rocks of the Omineca Mountains; *Geological Survey of Canada*, Paper 74-1A, pages 19-20.

Monger, J.W.H., Wheeler, J.O., Tipper, H.W., Gabrielse, H., Harms, T., Struik, L.C., Campbell, R.B., Dodds, C.J., Gehrels, G.E. and O'Brien, J. (in press): Cordilleran Terranes, Chapter 8, Upper Devonian to Middle Jurassic Assemblages, *in* The Cordilleran Orogen: Canada, Gabrielse, H. and Yorath, C.J., Editors, *Geological Survey of Canada*, Geology of Canada, Number 4.

Nixon, G.T. (1990): Geology and Precious Metal Potential of Mafic-Ultramafic Rocks in British Columbia: Current Progress; *B.C. Ministry of Energy, Mines and Petroleum Resources*, Geological Fieldwork 1989, Paper 1990-1, this volume.

Nixon, G.T. and Rublee, V.J. (1988): Alaskan-type Ultramafic Rocks in British Columbia: New Concepts of the Structure of the Tulameen Complex; *B.C. Ministry of Energy, Mines and Petroleum Resources*, Geological Fieldwork 1987, Paper 1988-1, pages 281-294.

Nixon, G.T., Ash, C.H., Connelly, J.N. and Case, G. (1989a): Preliminary Geology and Noble Metal Geochemistry of the Polaris Mafic-Ultramafic Complex; *B.C. Ministry of Energy, Mines and Petroleum Resources*, Open File 1989-17.

——— (1989b): Alaskan-type Mafic-Ultramafic Rocks in British Columbia: The Gnat Lakes, Hickman, and Menard Creek Complexes; *B.C. Ministry of Energy, Mines and Petroleum Resources*, Geological Fieldwork 1988, Paper 1989-1, pages 429-442.

Nixon, G.T., Cabri, L.J. and LaFlamme, J.H.G. (1989c): Tulameen Placers 92H/7, 10: Origin of Platinum Nuggets in Tulameen Placers: A Mineral Chemistry Approach with Potential for Exploration; *B.C. Ministry of Energy, Mines and Petroleum Resources*, Exploration in British Columbia 1988, pages B83-B89.

Nixon, G.T., Hammack, J.L., Ash, C.H., Connelly, J.N., Case, G., Paterson, W.P.E. and Nuttall, C. (1990): Geology of the Polaris Ultramafic Complex; *B.C. Ministry of Energy, Mines and Petroleum Resources*, Open File 1990-13.

Richards, T.A. (1976a): McConnell Creek Map Area (94D/E), Geology; *Geological Survey of Canada*, Open File 342.

——— (1976b): Takla Group (Reports 10-16): McConnell Creek Map Area (94D, East Half), British Columbia; *Geological Survey of Canada*, Paper 76-1A, pages 43-50.

Roots, E.F. (1954): Geology and Mineral Deposits of Aiken Lake Map Area, British Columbia; *Geological Survey of Canada*, Memoir 274, 246 pages.

St. Louis, R.M., Nesbitt, B.E. and Morton, R.D. (1986): Geochemistry of Platinum Group Elements in the Tulameen Ultramafic Complex, Southern British Columbia; *Economic Geology*, Volume 81, pages 961-973.

Wanless, R.K., Stevens, R.D., Lachance, G.R. and Edmonds, C.M. (1968): Age Determinations and Geologic Studies, K-Ar Isotopic Ages, Report 8; *Geological Survey of Canada*, Paper 67-2A, 141 pages.

Wheeler, J.O. and McFeely, P. (1987): Tectonic Assemblage Map of the Canadian Cordillera and Adjacent Parts of the United States of America; *Geological Survey of Canada*, Open File 1565.

Wheeler, J.O., Brookfield, A.J., Gabrielse, H., Monger, J.W.H., Tipper, H.W. and Woodsworth, G.J. (1988): Terrane Map of the Canadian Cordillera, *Geological Survey of Canada*, Open File 1894.

Woodsworth, G.J., Anderson, R.G., Armstrong, R.L., Struik, L.C. and Van der Heyden, P. (in press): Plutonic Regimes, Chapter 15, *in* The Cordilleran Orogen: Canada, Gabrielse, H. and Yorath, C.J., Editors, *Geological Survey of Canada*, Geology of Canada, Number 4.